Optical fibers applied to aerospace systems prognostics: Design and development of new FBG-based vibration sensors

# Optical fibers applied to aerospace systems prognostics: design and development of new FBG-based vibration sensors

# Optical fibers applied to aerospace systems prognostics: design and development of new FBG-based vibration sensors

**G Quattrocchi[1], P C Berri[1], M D L Dalla Vedova[1] and P Maggiore[1]**

[1] Department of Mechanics and Aerospace, Politecnico di Torino, Turin 10129, Italy

E-mail: gaetano.quattrocchi@polito.it

**Abstract.** Future generation actuation systems will be characterized by ever-increasing complexity. In this context, it will be necessary to adopt advanced health monitoring strategies to guarantee a high level of operational safety and system reliability. Prognostics and Health Management (PHM) is thus emerging as an enabling discipline for the design and operation of future advanced, complex systems. Smart systems with embedded self-monitoring capabilities are nowadays required in order to provide early faults identification and to perform innovative diagnostic and prognostic functions. In aerospace applications, the use of smart sensors could replace various types of traditional sensing elements, commonly used in structural monitoring with the additional capability of performing some prognostics or diagnostics tasks. This work proposes the first results of an experimental campaign aimed at evaluating and validating various packaging solutions for vibration amplification and detection using optical sensors (Fiber Bragg Gratings, FBGs), since characteristics frequencies can be good prognostics indicators of particular failure modes of a system. Several test samples were created by using 3D printed PLA and compared using a variety of bench tests. Results were compared in order to identify the strengths and weaknesses of the various proposed configurations, and were validated by comparing them with numerical simulations and experimental measurements performed with traditional sensors such as strain gages and accelerometers.

## 1. Introduction

In recent years, the development of optical fibers and relative components as cheap medium for data transmission [1] has enabled novel applications and has widened the potential plethora of users and adopters of the technology. One promising application of optical fibers is in aircraft data backbone [2], particularly military, given the extremely high data bandwidth that can be supported (up to Tb/s) on a single fiber, and the extremely useful characteristics of EMI immunity, since optical signals are not affected by electromagnetic jamming. Furthermore, fiber-based sensors can be used as structural monitoring tools as in [3], and for aging aircraft as in [4] .

At the same time, the development of computational capabilities of modern hardware has allowed continuous development of prognostics, defined as *the engineering discipline focused on predicting the time at which a system or a component will no longer perform its intended function* [5], especially leveraging machine learning techniques such as neural networks or metaheuristic algorithms.

In this context, the usefulness of optical-based sensors has emerged; Fiber Bragg Gratings (FBGs) offer a very promising technology for several applications, such as temperature measurement [6, 7], strain gauges [8, 9] and vibration sensors [10, 11]. FBGs operate on the principle of constructive phase interference, in association with Fresnel reflection. In essence, such sensors are periodical variations of refractive index 'inscribed' in the core of a single mode fiber, by using UV light interference [12], thus allowing a direct correlation between Bragg wavelength (peak reflected wavelength) and physical status of the grating, as visible in Fig. 1.

In this work, several fiber supports have been tested as narrow-band amplifiers for particular frequencies that can be seen as prognostics indicators given the correlation with particular modes of failures.

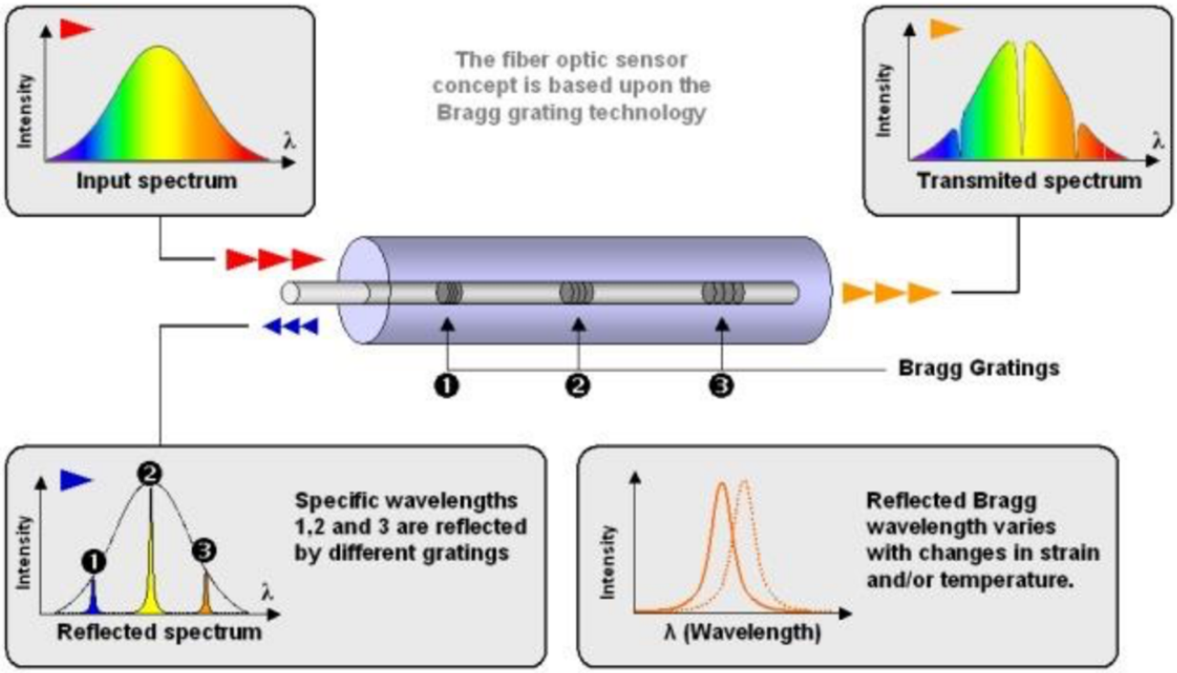


**Figure 1.** FBG sensors principle of operation

## 2. Data and experimental setup

Three different support (Figures 2, 3, 4) have been used for the testing campaign, all made of 3D printed PLA using FDM technology. Relevant data can be found in Table 1.

It has to be noted that pre-tensioning has been altered for combination 1-A, probably due to cyanoacrylate glue yielding and for combination 4-B probably due to initial excessive pre-tensioning and thus partial PLA yielding. The discrepancies have been observed before the start of the testing campaign, so the lower values have been used.

Furthermore, fiber 2 failed in early stages of pre-testing, so support B has been reused in combination with a new fiber, so the three fiber-support combinations evaluated in the testing campaign have been 1-A, 3-C and 4-B.

The experimental setup can be divided in two groups, the detection equipment (Fig. 5) and the excitation equipment (Fig. 6). The detection is carried by an opto-electronical interrogator, that is a device able to send a wide-band laser pulse along the fiber and detect with high precision the reflected spectrum.

| Fiber - support | Free length [mm] | Pre-tension [$\mu$strain], approx. | Fiber natural freq. [Hz] | Support natural freq. [HZ], FEM |
|---|---|---|---|---|
| 1 - A | 40 | 1600 $\rightarrow$ 1000 | 2360 | 1820 |
| 2 - B | 40 | 500 | 900 | 794 |
| 3 - C | 100 | 500 | 350 | 978 |
| 4 - B | 40 | 4200 $\rightarrow$ 2200 | 2330 | 794 |

**Table 1.** Support and fibers data

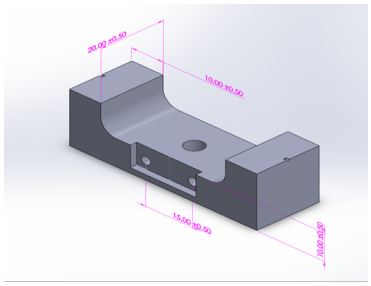

Support A

**Figure 2.** Support A schematics.

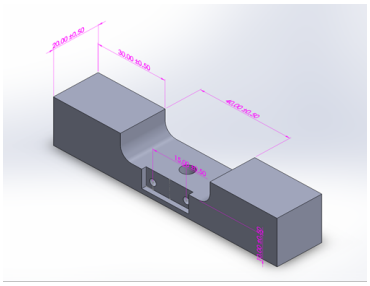

Support B

**Figure 3.** Suport B schematics.

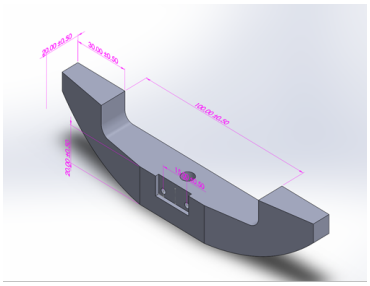

Support C

**Figure 4.** Support C schematics.

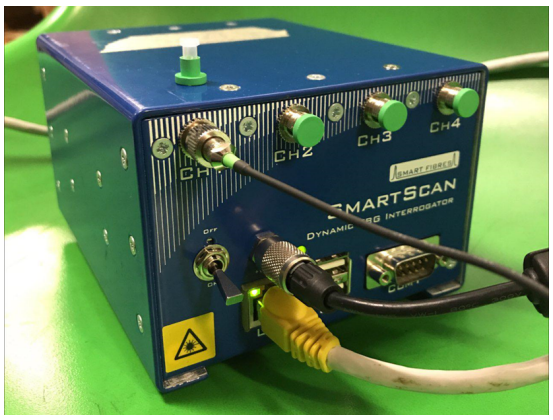


**Figure 5.** Experimental setup (1)

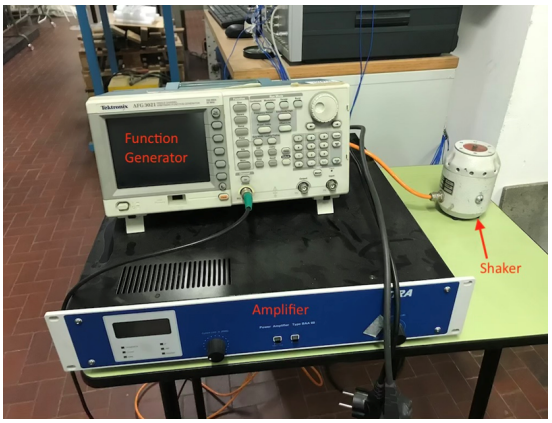


**Figure 6.** Experimental setup (2)

The excitation setup consist in a function generator used to generate a sine wave with desired frequency, an amplifier to increase the signal and a shaker where the support is mounted.

In Fig. 7 the setup during operation can be observed. Fiber is vibrating macroscopically, while no visible oscillation of the support is detectable. The element mounted on top of the support is an accelerometer used for close-loop control of the system.

An example of frequency analysis can be seen in Fig. 8, where the forcing frequency at 350 Hz is clearly visible but also higher order harmonics are detected. In particular, the second order harmonics is associated with the vibrating fiber at a frequency that is twice of that of the support. In this work, only the magnitude of the fundamental peak will be analysed.

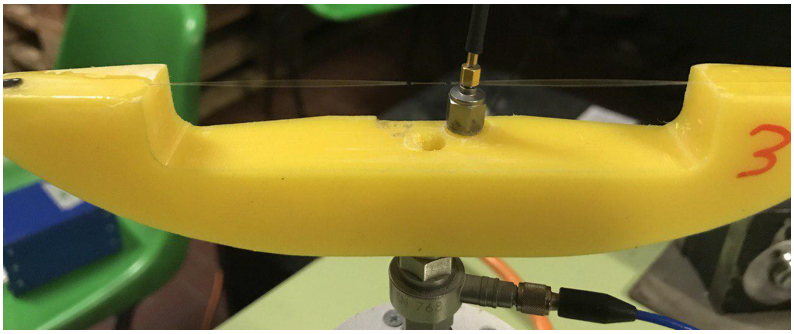


**Figure 7.** Experimental setup (3)

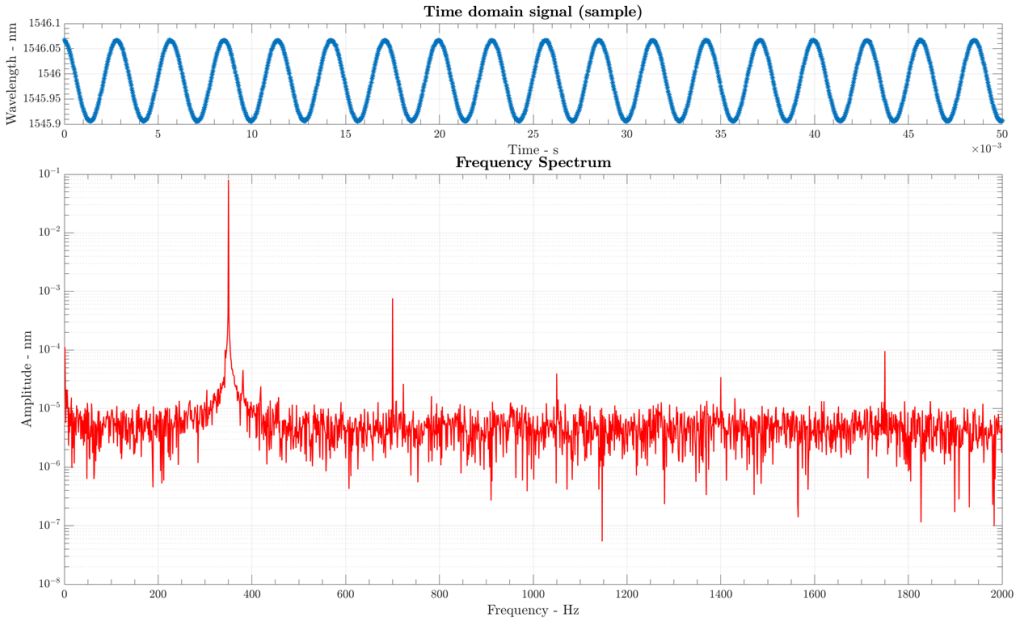


**Figure 8.** Frequency analysis of a sinusoidal excitation at 350 Hz.

## 3. Results

The results obtained will now be described. Fig. 9, 10 and 11 have all been obtained using constant acceleration of 1 $m/s^2$ as read by the accelerometer. On the other hand, Fig. 12, 13 and 14 have been obtained by setting output acceleration at 1, 5 and 20 $m/s^2$.

### *3.1. Constant amplitude*

The first graph, Fig. 9 is obtained for combination 1-A. The natural frequency is experimentally determined to be around 2200 Hz, substantially different between measured and predicted FEM frequency (1820 Hz). This discrepancy is probably due to incorrect meshing in the FEM analysis.

Figure 10 is relative to support B. In this case, resonance is clearly observed at circa 800 Hz, a very similar value to the FEM solution, with a relatively narrow amplification band.

Finally, for support C (Fig. 11), a similar behaviour as support B is observed. The experimentally determined resonance agrees with what obtained with FEM analysis, with resonance around 1000 Hz.

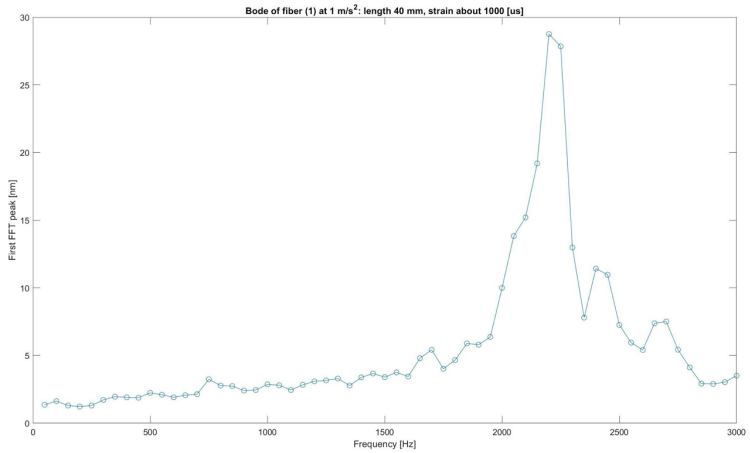


**Figure 9.** Bode plot – Support A

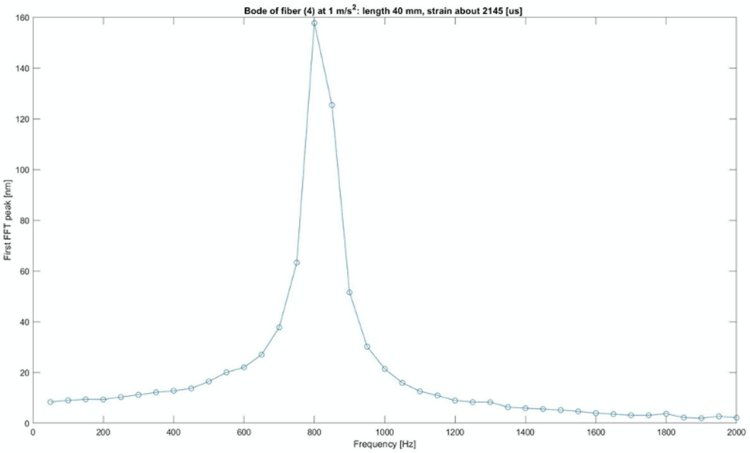


**Figure 10.** Bode plot – Support B

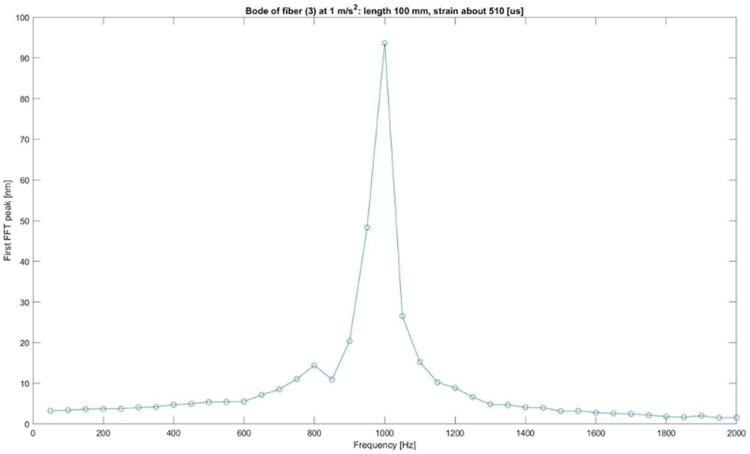


**Figure 11.** Bode plot – Support C

*3.2. Varying amplitude*

After a constant amplitude testing (at 1 $m/s^2$) for every support, each support has been tested at varying amplitude.

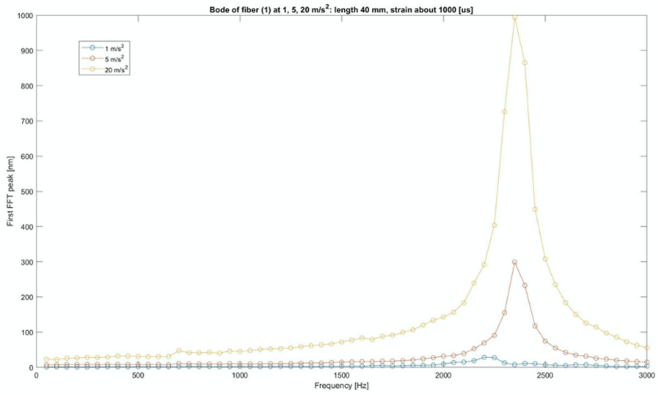


**Figure 12.** Bode plots at varying amplitude - Support A

In Fig. 12, three Bode plots for support A are shown. There is a proportionality between the response and amplitude of the forcing function, while the resonance peak seems to be consistently observed around the same value.

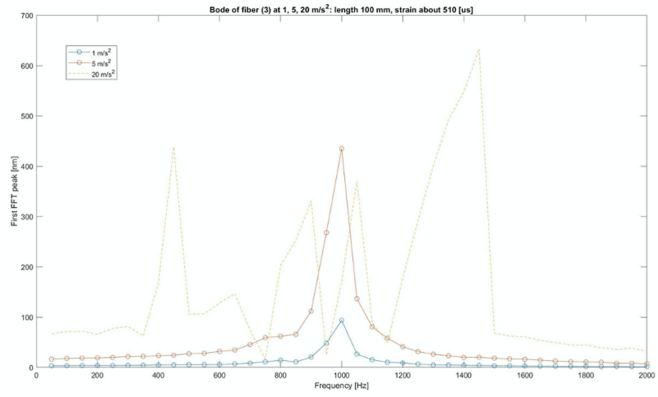


**Figure 13.** Bode plots at varying amplitude - Support B

For support B (Fig. 13), the measurement at highest amplitude has clearly been affected by some kind of setup error, so the data obtained are not relevant. On the other hand, the measurements at 1 and 5 $m/s^2$ shows proportionality and the resonance frequency remains at around 1000 Hz and does not seem to vary with amplitude.

Finally, for support C, there is an anomaly detected for the highest amplitude Bode, that is an amplitude around the resonance frequency that is too low; furthermore, a shift in resonance frequency to lower values with an increase of amplitude is observed, thus implying non linear effects, probably due to material non-linearities.

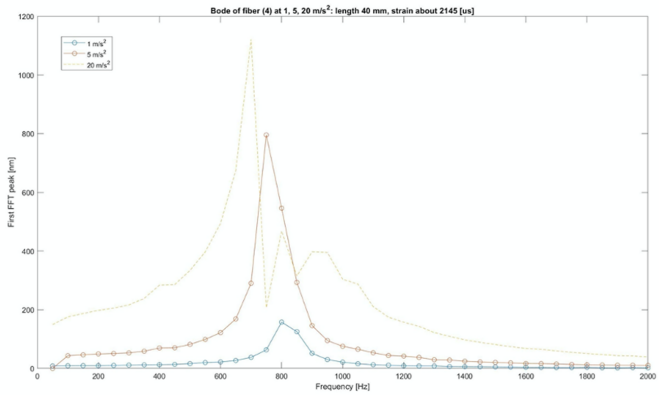


**Figure 14.** Bode plots at varying amplitude - Support C

## 4. Conclusions and future works

This work has shown that supports can be designed in order to resonate at a given frequency, strongly increasing FBG sensitivity, and this is particularly useful since small amplitude vibration in mechanical systems need to be detected in order to have proper early prognostics and thus an effective system health indication and in order to correctly plan for condition-based maintenance.

Several flaws have been observed in the setup that will need to be corrected in future works. Firstly, the bonding technique adopted for fibers and supports is clearly perfectible, given the fact that slippage has been detected in two samples; furthermore, the non-linearities of the glue need to be quantified and included in the design phase. The effect of humidity and temperature on the measurements will also need to be studied, as in [13].

Several measurements at moderately high amplitude (20 $m/s^2$) have yielded inconclusive results, so those measurements need to be repeated and the origins of measurement errors need to be pinpointed.

Finally, an analysis on the fiber resonance, that is the second peak observed in the frequency domain corresponding to two times the excitation frequency. This phenomenon could be leveraged as amplifier for another frequency of interest if the support is properly designed.

## References

[1] Inigo Artundo et al. “Cost forecasting of passive components for optical fiber network deployments”. In: *Optical Fiber Technology* 17.3 (2011), pp. 218–226.

[2] Sarry F Habiby and Ravi Vaidyanathan. “WDM optical backbone networks in aircraft applications: Networking challenges and standards progress”. In: *MILCOM 2009-2009 IEEE Military Communications Conference*. IEEE. 2009, pp. 1–6.

[3] Iker García et al. “Optical fiber sensors for aircraft structural health monitoring”. In: *Sensors* 15.7 (2015), pp. 15494–15519.

[4] KR Cooper et al. “Optical fiber-based corrosion sensor systems for health monitoring of aging aircraft”. In: *2001 IEEE Autotestcon Proceedings. IEEE Systems Readiness Technology Conference.(Cat. No. 01CH37237)*. IEEE. 2001, pp. 847–856.

[5] George Z Vachtsevanos. *Intelligent fault diagnosis and prognosis for engineering systems*. John Wiley & Sons, 2006.

[6] Bowei Zhang and Mojtaba Kahrizi. “High-temperature resistance fiber Bragg grating temperature sensor fabrication”. In: *IEEE sensors journal* 7.4 (2007), pp. 586–591.

[7] Tianliang Li et al. "A non-contact FBG vibration sensor with double differential temperature compensation". In: *Optical Review* 23.1 (2016), pp. 26–32.

[8] Daniel C Betz et al. "Advanced layout of a fiber Bragg grating strain gauge rosette". In: *Journal of lightwave technology* 24.2 (2006), pp. 1019–1026.

[9] Frank M Haran, Jason K Rew, and Peter D Foote. "Fiber Bragg grating strain gauge rosette with temperature compensation". In: *Smart Structures and Materials 1998: Sensory Phenomena and Measurement Instrumentation for Smart Structures and Materials*. Vol. 3330. International Society for Optics and Photonics. 1998, pp. 220–230.

[10] Yinyan Weng et al. "A robust and compact fiber Bragg grating vibration sensor for seismic measurement". In: *IEEE sensors journal* 12.4 (2011), pp. 800–804.

[11] Satoshi Tanaka et al. "Thermally stabilized fiber-Bragg-grating vibration sensor using erbium-doped fiber laser". In: *Japanese journal of applied physics* 42.5S (2003), p. 3060.

[12] G Meltz, W W Morey, and WH Glenn. "Formation of Bragg gratings in optical fibers by a transverse holographic method". In: *Optics letters* 14.15 (1989), pp. 823–825.

[13] PC Berri et al. "Feasibility study of FBG-based sensors for prognostics in aerospace applications". In: *Journal of Physics: Conference Series*. Vol. 1249. 1. IOP Publishing. 2019, p. 012015.